

Generic models of the biomass of larches (*Larix* spp.) and stone pines (*Pinus* L. subsection *Cembrae* Loud.) for laser sensing in climatic gradients of Eurasia

Vladimir Andreevich Usoltsev^{1,2}, Walery Zukow^{3*}, Ivan Stepanovich Tsepordey²

¹Ural State Forest Engineering University, str. Sibirskiy Trakt, 37, 620100 Yekaterinburg, Russia

²Botanical Garden of Ural Branch of RAS, str. 8 Marta, 202a, 620144 Yekaterinburg, Russia

³Faculty of Earth Sciences and Spatial Management, Nicolaus Copernicus University, str. Lwowska 1, 87-100 Toruń, Poland

*corresponding author e-mail: zukow@wp.pl

Received: 20 March 2021 / Accepted: 28 April 2021

Abstract. In the context of growing global urbanization and climate fluctuations, understanding the development of forest ecosystems in terms of their ability to remove atmospheric carbon is of increasing interest. Its content in the atmosphere continues to increase due to the burning of fossil fuels and deforestation. Airborne laser scanning technology has become widely used in assessing the biomass of trees by remotely registering such taxation indicators of trees, such as the width of the crown and the height of the tree. There are many allometric biomass models of different tree species in different climatic conditions, but allometric models for estimating biomass by remote methods are presented by single works.

The authors use the base of harvest data of 138 sample trees of larch (*Larix* spp.) and 93 ones of stone pines (*Pinus* L. subsection *Cembrae* Loud.) growing on Eurasia with measured indicators of tree height, crown width, as well as the biomass of the trunk, foliage, branches and roots. For all components of aboveground biomass, a positive relationship with the crown width and the tree height was established.

The results obtained give an vision of how the structure of the biomass of equal-sized trees of such species as larch and stone pine can differ, whether this structure can change in the climatic gradients of Eurasia, what can be the contribution of climate variables to the explanation of the variability of tree biomass, and what are the potential possibilities of laser technology for recognizing tree species at the level of individual trees.

Keywords: hydrothermal gradients, biomass components; laser sensing of trees, allometric models, average January temperature, annual precipitation.

1. Introduction

In the context of growing global urbanization and climate fluctuations, understanding the development of forest ecosystems in terms of their ability to absorb atmospheric carbon is of increasing interest. Carbon content in the atmosphere continues to increase due to the burning of fossil fuels and deforestation (Colombo, 2008). Due to the complexity of the morphometric structure of forest communities, predictive models that reflect their response to climate change need to take into account not only environmental factors, but also the structural parameters of trees and stands (Grote et al., 2011). With the current extremely rapid changes in the technical and software support of remote sensing methods for forest ecosystems, the assessment of their biomass and carbon deposition capacity is becoming quite feasible. The possibility of

such estimates largely depends on the rapid and fairly correct assessment of the structural parameters of the tree canopy, and first of all, the crown sizes and the tree height.

In recent years, significant advances have been made in the field of individual tree detection and recording of crown shape and structure (crown width, crown projection area and volume, tree height) based on new high-performance algorithms and the use of unmanned aerial vehicles (UAVs, or drones) (Lefsky et al., 2003; Hyypä et al., 2008; Dalponte, 2018; Goodwin et al., 2006; Jing et al., 2012; Neuville et al., 2021). The airborne laser sensor measures the distance to the structural elements of a tree and to the ground, recording the time interval between the emission and the return of laser pulses (Lefsky et al., 2003). In recent years, a fundamentally new laser-location method for shooting the forest canopy has appeared, which allows processing huge amounts of laser sensing data in real time, almost simultaneously with making measurements, not only of the total forest cover, but also of the totality of individual trees (Næsset & Økland, 2002; Danilin et al., 2005; Ørka et al., 2009; Hayashi, 2014). Thus, significant progress in assessing the biomass and carbon-depositing capacity of forest ecosystems today can be achieved by laser registration from UAVs, primarily, such structural elements of a tree as the crown width and the tree height, which determine the structure of the tree biomass.

As early as the end of the XIX century, R. Hartig, using 52-year-old spruce trees, showed that with a change in the crown width in the range from 1.5 to 3.0 m, the biomass of the green shoots increases from 15 to 119 kg (Hartig, 1896). A similar pattern was later shown by A. Dengler on the example of Scots pine at the age of 150-160 years: with a change in the crown projection area in the range from 10 to 71 m², the needle biomass of a tree increases from 8.0 to 51.4 kg (Dengler, 1937). Already the first attempts of correlation analysis of the mass of spruce and fir needles of different ages and the projection area of the tree crown showed the presence of a close relationship between these indicators, while the correlation coefficient varied from 0.91 to 0.97 (Kern, 1962). Having analyzed the relationship between the foliage biomass and various parameters of the crown on the example of 26 hinoki (*Chamaecyparis obtusa*) trees aged from 9 to 76 years, M. Kajihara (1981) found that this relationship with the area of the crown projection is less close than with the volume of the crown mantle (its foliated part) ($0.849 < 0.906$). He obtained a similar conclusion for sugi (*Cryptomeria japonica*) (Kajihara, 1980). Attempts were also made to relate the crown biomass to its volume (Burger, 1939; Kern, 1962; Westman & Whittaker, 1975), but due to the complexity and lack of accuracy in determining the crown volume, they were not developed. For three climatic zones of Siberia, using extensive harvest data, the dependence of the crown biomass of Scots pine on the crown width was proposed (Pozdnyakov et al., 1969).

Unfortunately, subsequent studies under the International Biological Program and other environmental programs did not pay sufficient attention to the assessment of crown parameters as predictors of tree biomass. When processing model trees on the sample plots, the researchers usually took into account tree age, height, and stem diameter at breast height (DBH), since their totality explained 90-99% of the variability of a particular component of the biomass in ground-based taxation.

Sometimes the distance from the stem base to the crown base was also measured, but rarely the crown width was measured. In addition, due to the irregular shape of the crown projection, the accuracy of measuring crown width was questionable, in any case, much lower than the accuracy of measuring the DBH. It was believed that the crown width does not significantly contribute to the explanation of the variability of the tree's biomass, and the main contribution is provided by the DBH. Today, the proportion of model trees with measured crown width and tree height in their total number is from 10 to 30 % in different tree species. For example, for alder in Eurasia, there are definitions of aboveground biomass in relation to the DBH - 62, in relation to DBH, tree height and crown width – only 23, and the root biomass of alder is determined only in 4 trees (Kapustinskaite & Rusečkas, 1982; Usoltsev, 2016).

Currently, the basis for estimating forest biomass is its allometric dependences on DBH and, more rarely, on DBH and tree height, and thousands of such models have been published for hundreds of tree species. For example, about 6,000 such allometric models of tree biomass have been published for China alone (Luo et al., 2020). As far as we know, similar allometric models designed to determine the biomass by remote registration of the crown width and height of trees are rare and extremely insufficient in the literature (Goodman et al., 2014; Jucker et al., 2017; Lau et al., 2019; Usoltsev et al., 2019a; Machimura et al., 2021). This vacuum should be filled as soon as possible due to the obvious prospects for assessing forest biomass using laser sensing techniques.

Since trees of different species have a specific crown configuration, this specificity is now successfully recognized using airborne and ground-based laser sensors (Puttonen et al., 2011; Zhen et al., 2016; Åkerblom et al., 2017; Calders et al., 2020; Van Den Berge et al., 2021). With multiple registration of reflected laser pulses, it is possible to successfully distinguish plant species by the pattern of grouping of point clouds of the crown profile and its outline (Næsset et al., 2004; Puttonen et al., 2010; Zhang & Hu, 2012).

An effective method of vegetation remote sensing is the laser identification of tree species based on measurements of spectral brightness and reflection coefficients (Belov & Artsybashev, 1957; Jaaskelainen et al., 1994; Atkinson et al., 1997; Martin et al., 1998; Knight et al., 2004; Sobhan, 2007). Forests are usually represented by combinations of different species of different ages, and different physiological conditions. This results in significant intraspecific spectral variability (Jensen, 2005). The solution is provided by artificial intelligence methods, such as the logic of fuzzy sets and neural networks. They are widely used in multispectral analysis of laser images (Mas & Flores, 2008; Hyyppä et al., 2008; Voss & Sugumaran, 2008; Dalponte et al., 2008).

A neural network approach has been developed to identify tree species at the level of individual trees from lidar and hyperspectral images. It is shown that lidar data combined with hyperspectral images can not only detect individual trees and determine the size of tree crowns, but also simultaneously identify several tree species using the developed algorithm. The consequence of integrating these two data sources is that they can replace traditional field measurements (Oki et al., 2006; Zhang & Qiu, 2012; Hennessy et al., 2020). In addition, the labor-consuming

traditional technology of ground-based assessment of stand biomass on sample plots using allometric models is now being successfully replaced by ground-based laser scanning technology (Campbell & Borden, 2005; Blanchette et al., 2015) and spherical image technology. Of these, the latter is characterized by increased accuracy, significant time and cost savings (Dai, 2021).

At the current rate of development of laser and IT-tools, it is possible to distinguish between such coniferous species as deciduous larch and evergreen stone pine. Lidar from a flying drone will be able to distinguish them in the summer by different spectral brightness (Belov & Artsybashev, 1957; Masaitis et al., 2013; Tolkach & Sayevich, 2016; Neuville et al., 2021). In winter, the monopodial structure of the larch crown is distinguished from the sympodial structures of deciduous leaved species by the specific grouping of laser pulses in the tree crown profile (Shlyakhter et al., 2001; Huang & Mayer, 2007).

The crown width indicator was used to estimate the aboveground biomass of multi-stemmed trees and shrubs instead of the DBH, since in such cases the DBH was difficult to measure and not informative enough (Leontiev, 1950; Ohmann et al., 1976). In particular, two-factor allometric models relating aboveground biomass to the tree (bush) height and the crown width were developed for saxaul (*Haloxylon Bunge*) growing in the deserts of Central Asia (Veyisov & Kaplin, 1976):

$$\ln P_a = a_0 + a_1 \ln D_{cr} + a_2 \ln H, \quad (1)$$

where P_a is aboveground biomass, kg; D_{cr} is crown width, m; H is brush height, m.

The involving temperature and precipitation as additional independent variables in allometric models of biomass significantly improved the accuracy of estimates and made it possible to predict changes in biomass during climate shifts (Fu et al., 2017; Zeng et al., 2017). However, the models were developed for the aboveground biomass of trees as a whole, without dividing it into components, without taking into account the crown width, and did not take into account the contribution of climate variables to the explanation of biomass variability.

In the proposed study, we intend to: (1) determine whether there are statistically significant differences in the biomass structure determined by the crown width and tree height between deciduous larches and evergreen five-needled (stone) pine, (2) find out how the components of biomass relate not only to the taxation indicators of trees, but also to temperature and precipitation fluctuations in Eurasia, and (3) what contribution to the explanation of the variability of the components of biomass is made by the taxation indicators of trees, species affiliation and climate variables.

2. Materials and methods

To solve these problems, we used the author's base of harvest data on the biomass of trees of forest-forming species of Eurasia in the amount of 15,200 trees (Usoltsev, 2020). From it, 138 and 93 model trees were selected, respectively, larches (*Larix* spp.) and five-needled (stone) pines (*Pinus* L. subsection *Cembrae* Loud.) with

measured taxation and biomass indicators (Table 1). The genus *Larix* spp. is represented by the species *L. decidua* Mill., *L. sibirica* L., *L. cajanderi* Mayr., *L. gmelinii* (Rupr.) Rupr., *L. leptolepis* Gord. Five-needled (stone) pines are represented by two species: mainly *Pinus sibirica* Du Tour. and to a lesser extent *P. koraiensis* S. et Z. The experimental material was processed using the Statgraphics software (<http://www.statgraphics.com/>).

Table 1. Statistics of database samples for larches and stone pines in Eurasia

Statistic designation*	Indices analyzed(**)							
	<i>H</i>	<i>Dcr</i>	<i>Ps</i>	<i>Pb</i>	<i>Pf</i>	<i>Pa</i>	<i>Pr</i>	<i>Pr/Pa</i>
Larch (<i>Larix</i> spp.)								
Mean	12.8	3.2	114.0	16.6	2.8	133.45	69.5	0.32
Min	1.4	0.3	0.01	0.004	0.004	0.02	1.66	0.08
Max	34.0	13.0	1964.6	448.3	35.1	2447.9	768.4	0.78
SD	6.6	2.0	230.7	42.9	4.3	274.3	131.6	0.15
CV,%	51.5	61.0	202.3	258.3	152.6	205.5	189.2	45.9
n	138.0	138.0	138.0	138.0	138.0	138.0	66.0	66.0
Stone pine (<i>Pinus</i> L. subsection <i>Cembrae</i> Loud.)								
Mean	7.9	2.4	49.2	10.3	4.9	64.5	-	-
Min	1.5	0.35	0.24	0.09	0.03	0.73	-	-
Max	26.8	7.7	724.5	135.5	47.7	904.2	-	-
SD	6.4	1.5	129.9	23.9	9.4	162.2	-	-
CV,%	80.7	60.9	263.8	231.7	191.6	251.6	-	-
n	93.0	93.0	93.0	93.0	93.0	93.0	1.0	1.0

*Min=minimum, Max=maximum, SD=standard deviation, CV=coefficient of variation, n=number of observations.

(**) *Ps*, *Pb*, *Pf*, *Pa*, *Pr* = stem over bark, branches, foliage, aboveground, root biomass in a completely dry condition correspondingly, kg.

3. Results and discussion

Based on the analysis of published data (Ohmann et al., 1976; Veyisov & Kaplin, 1976; Fu & Wu, 2011; Lines et al., 2012; Goodman et al., 2014; Usoltsev et al., 2019a), we concluded that the most informative independent variables in estimating tree biomass by remote sensing are the crown width and tree height according to model (1), and it is possible to do without measuring the DBH (Jucker et al., 2017).

The structure of the two-factor allometric model is adopted:

$$\ln P_i = a_0 + a_1(\ln Dcr) + a_2(\ln H) + a_3 X, \quad (2)$$

where P_i = biomass i -th tree component. In order to reveal the difference between larch and stone pine in tree biomass (or its absence), the binary variable X is introduced in the model (2) as an additional independent variable, which encodes data for larch ($X = 0$) and stone pine ($X = 1$). The results of calculating the model (2) are shown in Table 2.

Table 2. Results of calculation of the model (2)

	Dependent variables			
	$\ln Ps$	$\ln Pf$	$\ln Pb$	$\ln Pa$
a_0^*	-3.0209	-2.9697	-2.7930	-2.1092
$\ln Dcr$	0.9126	1.7579	1.8346	1.1370
$\ln H$	2.3268	0.6608	1.1064	1.9513
X	0.1028	1.1570	0.4516	0.2477
$adjR^2$	0.962	0.838	0.905	0.950
SE	0.43	0.64	0.59	0.46

*The intercept hereafter is adjusted according to Baskerville's (1972) logarithmic transformation; $adjR^2$ = the coefficient of determination, adjusted for the number of variables; SE = the standard error of the equation.

The binary variable X in model (2) is significant at the level of $p < 0.001$. The exception is the binary variable of the model for stem biomass ($t = 1.60 < t_{95} = 1.96$). The binary variable for all components of the biomass has a plus sign, which means that for the same values of tree height and crown width, the biomass of all aboveground components in stone pines is significantly greater than in larches.

To answer the second question of our study, the available data of the geographical coordinates of the model trees are plotted on the maps of the average January temperature (https://store.mapsofworld.com/image/cache/data/map_2014/currents-and-temperature-jan-enlarge-900x700.jpg) and average annual precipitation (<http://www.mapmost.com/world-precipitation-map/free-world-precipitation-map/>) (World Weather Maps, 2007) (Figs 1 and 2) and were simultaneously combined with the taxation and biomass indicators of trees in one common matrix (Usoltsev et al., 2020a), which was then included in the regression analysis procedure (Usoltsev et al., 2019b). The rejection of the use of the average annual temperature in favor of the average January temperature was justified earlier (Usoltsev et al., 2019b; 2020a).

Based on the fulfilled analysis, the structure of the model is proposed, which includes both morphometric characteristics of trees and climatic indicators as independent variables:

$$\ln P_i = a_0 + a_1(\ln Dcr) + a_2(\ln H) + a_3X + a_4[\ln(T+40)] + a_5(\ln PR) + a_6[\ln(T+40)] \cdot (\ln PR), \quad (3)$$

where T is average January temperature, °C; PR is average annual precipitation, mm; $[\ln(T+40)] \cdot (\ln PR)$ is a combined variable that characterizes the joint effect of temperature and precipitation. Since the average temperature of January in high latitudes has a negative value, for its logarithm transforming in the model (3), it is modified to the form $(T+40)$.

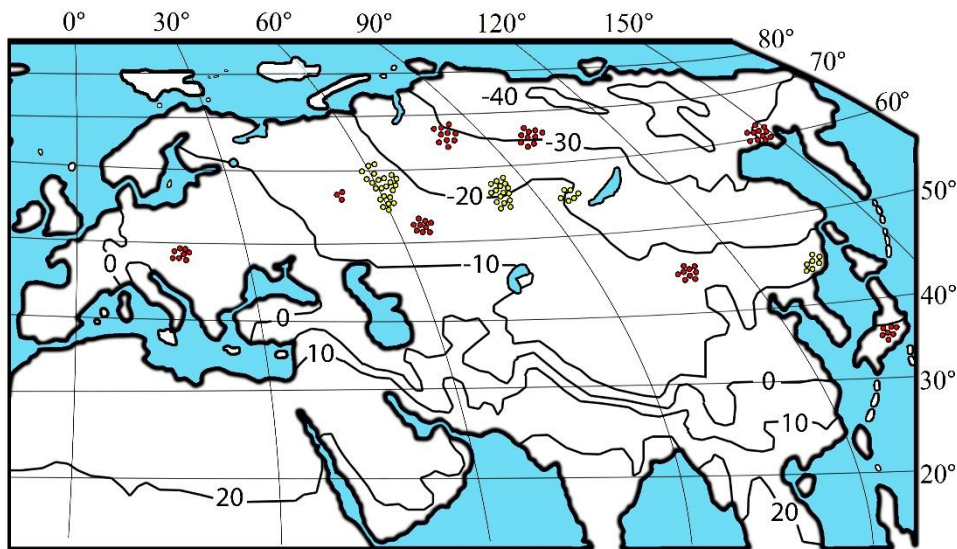


Figure 1. Allocation of the harvest biomass data of 138 и 93 larch (red circles) and stone pine (yellow circles) sample trees, respectively, on the map of January isotherms, °C (World Weather Maps, 2007)

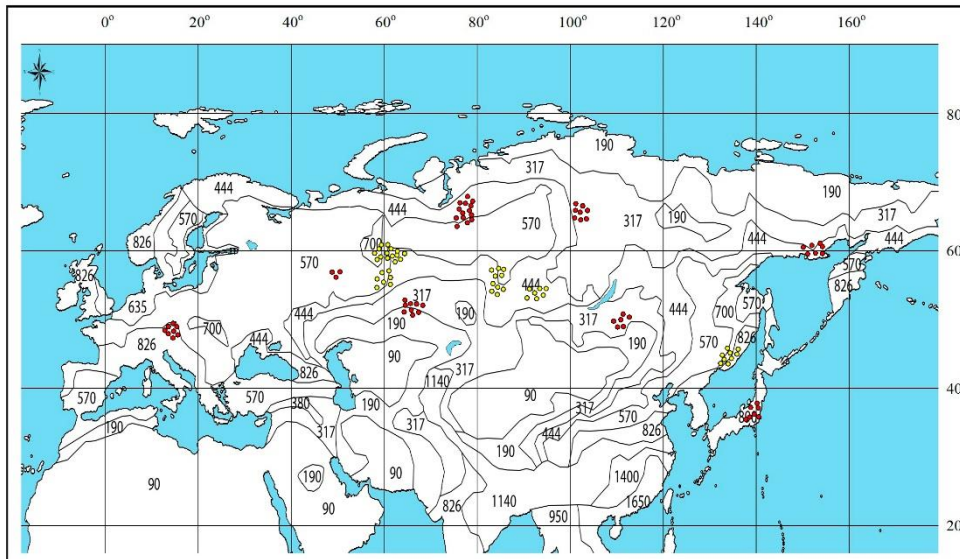


Figure 2. Allocation of the harvest biomass data of 138 и 93 larch (red circles) and stone pine (yellow circles) sample trees, respectively, on the map of annual precipitation, mm (World Weather Maps, 2007).

The mentioned database (Usoltsev, 2020) contains 790 and 170 model trees of larch and stone pine, respectively, with measured values of the component composition of the biomass, as well as the age, height and DBH of trees. As it was mentioned above, the harvest data containing the values of biomass and crown width are usually significantly less than the biomass and measurements of the tree stem. As can be seen in Table 1, we were able to include in our analysis only 138 and 93 model larch and stone pine trees with crown width measurements, i.e. 6 and 2 times less, respectively, then there are in the database. Of the 138 and 93 model trees with crown width measurements, only 66 and 1 tree, respectively, had measured root biomass values. A similar disparity of aboveground and underground biomass data is typical

for all published databases on tree and stand biomass (Cannell, 1982; Falster et al., 2015; Schepaschenko et al., 2017). Due to the insufficient representation of data on the root biomass, we calculate models (3) for the relative indicator, namely for Pr/Pa , and combine both species into one general model, encoding them with the binary variable X .

The results of calculating the models (3) are shown in Table 3.

Table 3. The results of calculating the models (3)

$\ln(Y)$	a_0	$\ln Dcr$	$\ln H$	X	$\ln(T+40)$	$\ln PR$	$[\ln(T+40)] \times (\ln PR)$	adjR ²	SE
$\ln(Ps)$	-13.0615	0.9349	2.3019	0.0222	3.1012 ^(*)	1.6365 ^(*)	-0.5001 ^(*)	0.962	0.43
$\ln(Pf)$	5.8853	1.7812	0.7572	1.3459	-1.6279 ^(*)	-1.5105 ^(*)	0.2729 ^(*)	0.848	0.63
$\ln(Pb)$	-22.7574	1.8804	1.0617	0.2980	6.2132	3.2550	-1.0031	0.907	0.58
$\ln(Pa)$	-16.0726	1.1690	1.9166	0.1362	4.3287	2.2717	-0.6968	0.951	0.45
$\ln(Pr/Pa)$	-0.4742	0.9447	-0.7325	-	-	-	-	0.463	0.35

^(*)Regression coefficients are not significant at $p < 0.05$.

The regression coefficients of the models presented in Table 3 are significant at the level of $p < 0.001$, with the exception of the variables marked as (*) for the biomass of stems and foliage, which are not significant at the level of $p < 0.05$. The geometric interpretation of models (3) (Fig. 3) for larch biomass is obtained by substituting in (3) the average H and Dcr values for larch taken from Table 1. Since we compare the biomass of two species under the condition of equal tree sizes, these sizes should be the same for both species.

As we can see in Figure 3, the dependence of all the biomass components of equal-sized larch trees upon temperature and precipitation is described by a propeller-shaped 3D surface. In cold regions, as precipitation increases, the biomass increases, but as one moves to warm regions, it is characterized by an opposite or neutral trend. As the temperature increases in wet regions, the biomass decreases, but as the transition to dry conditions, it increases or does not respond to temperature changes, as can be observed with respect to the needle biomass. During the transition from wet to dry conditions, the biomass of needles increases regardless of the level of annual precipitation. For stone pines, Figure 3 is repeated, but the 3D surfaces for the biomass of branches, trunks, and aboveground are shifted up along the ordinate axis according to models (3) by 35, 2, and 15%, respectively. Equal-sized stone pine trees have the needle biomass that is almost three times greater than that of larch.

In other woody species, in particular, two-needled pines, oak, spruce, and fir, the patterns sometimes differ in some components from those shown in Figure 3, and sometimes are opposite in all components (Usoltsev et al., 2019b; Usoltsev et al., 2020a, b). Apparently, this is due to the biological properties of tree species and to the peculiarities of the distribution of assimilates of the tree into its various components (Poorter et al., 2015; Zanutelli et al., 2013; Xiong et al., 2021; Liu et al., 2021; Rehling et al., 2021).

In the model for Pr/Pa , only the regression coefficients for $\ln Dcr$ ($t = 7.6 > t_{999} = 3.29$) and for $\ln H$ ($t = 5.0 > t_{999} = 3.29$) were significant (Fig. 4).

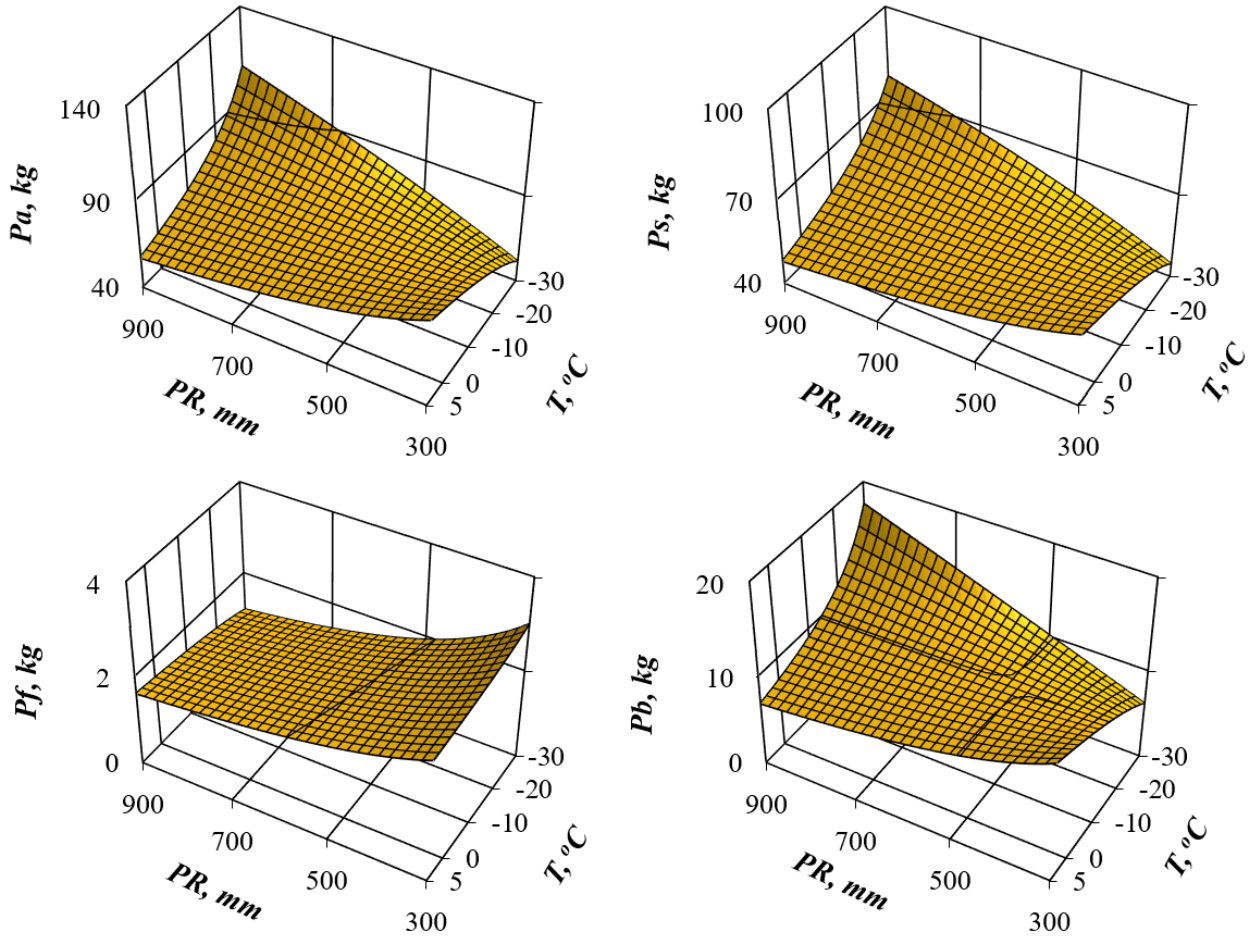


Figure 3. Relationships of larch biomass components with average January temperature (T) and average precipitation (PR). See Table 1 for the designations

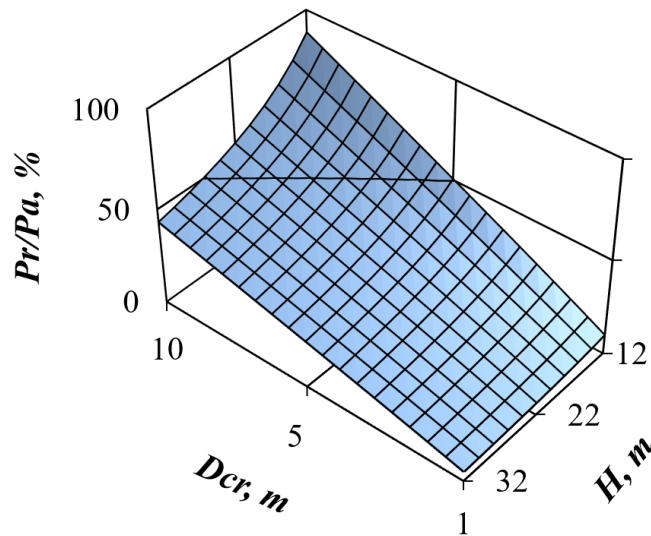


Figure 4. Dependence of the Pr/Pa ratio of larch and stone pine trees on the crown width and tree height

The answer to the third question of our study can be obtained from the data in Table 4.

Table 4. Contribution of the independent variables of equations (3) to the explanation of the variability of the dependent variables, %

ln(Y)	Independent variables							
	lnDcr (I)	lnH (II)	I+II	X	ln(Tm+40) (III)	lnPRm (IV)	[ln(Tm+40)] × (lnPRm) (V)	III+IV+ V
ln(Ps)	24.8	63.8	88.6	0.6	3.6	3.5	3.7	10.8
ln(Pf)	43.5	19.4	62.9	30.6	1.8	2.9	1.6	6.5
ln(Pb)	46.1	27.2	73.3	6.8	6.7	6.4	6.8	19.9
ln(Pa)	30.2	51.8	82.0	3.3	5.0	4.7	5.0	14.7
X ± σ ^(*)	36.2 ±10.3	40.6 ±20.8	76.7 ±11.1	10.3 ±13.8	4.3 ±2.1	4.4 ±1.5	4.3 ±2.2	13.0 ±5.7

^(*)X ± σ = mean value ± standard deviation.

We can see in Table 4 that the average contributions of tree taxation indices, species affiliation, and climate variables to the explanation of the variability of biomass components are 76.7, 10.3, and 13.0%, respectively. The contribution of the binary variable to the explanation of the variability of the biomass of the trunk, branches and aboveground is small and ranges from about 1 to 7%. The binary variable makes the greatest contribution to the explanation of the variability in the needle biomass (about 31%), which is consistent with an almost three-fold difference in the biomass of larch and stone pine needles of equal trees.

The results obtained should be considered as preliminary, in particular, due to the insufficient representation of harvest data in all temperature and precipitation ranges in Eurasia. For example, there are no harvest data on *Larix gmelinii* var. *olgensis* A. Henry, native to the Far East, and on *L. principis-rupprechtii* Mayr, *L. potaninii* Batal., *L. mastersiana* Rehd. et Wils., *L. griffithii* Hook. f. et Toms., native to central and southern China, for which only allometric models have been published (Luo et al., 2020). The natural growth area of stone pines is much smaller compared to larches, and the mentioned uncertainty about the change in its biomass in climatic gradients applies primarily to stone pines.

Nevertheless, the results provide an idea of how much the biomass structure of equal-sized trees of such species as larch and stone pine can differ, whether this structure can change in the climatic gradients of Eurasia, and what the contribution of climate variables to the explanation of the variability of tree biomass can be.

4. Conclusions

1. On the basis of the author's database on the biomass of larch and stone pine in Eurasia in the amount of 138 and 93 model trees, respectively, it was found that the above-ground biomass of trunks and branches of stone pine trees of equal crown width and equal tree height is 15, 2, and 35% more than that of larch.

According to the biomass of needles of trees, a three-fold excess of stone pine over larch was found.

2. The introduction of temperature and precipitation as additional independent variables into the allometric model showed that the biomass of equal-sized trees is described by a propeller-shaped 3D dependence. In cold regions, as precipitation increases, the biomass increases, but as one moves to warm regions, it is characterized by an opposite or neutral trend. As the temperature increases in wet regions, the biomass decreases, but as the transition to dry conditions it increases or does not respond to temperature changes, as can be observed with respect to the needle biomass. During the transition from wet to dry conditions, the biomass of needles increases regardless of the level of annual precipitation.
3. The average contribution of tree taxation indices, species affiliation, and climate variables to the explanation of the variability of biomass components is 77, 10, and 13%, respectively.
4. The results obtained can be useful in monitoring forest biomass based on laser sensing.

Acknowledgments

We thank the anonymous referees for their useful suggestions. This paper is fulfilled according to the programs of current scientific research of the Ural Forest Engineering University and Botanical Garden of the Ural Branch of Russian Academy of Sciences.

References

- Åkerblom M., Raunonen P., Mäkipää R. & Kaasalainen M., 2017, Automatic tree species recognition with quantitative structure models. *Remote Sensing of Environment* 191: 1–12.
- Atkinson M.D., Jervis A.P. & Sangha R.S., 1997, Discrimination between *Betula pendula*, *Betula pubescens*, and their hybrids using near-infrared reflectance spectroscopy. *Canadian Journal of Forest Research* 27: 1896-1900.
- Baskerville G.L., 1972, Use of logarithmic regression in the estimation of plant biomass. *Canadian Journal of Forest Research* 2(1): 49-53.
- Belov S.V. & Artsybashev E.S., 1957, Study of the reflectivity of wood species. *Botanical Journal [Botanicheskiy Zhurnal]* 42(4): 517-534 (in Russian).
- Blanchette D., Fournier R.A., Luther J.E. & Côté J.-F., 2015, Predicting wood fiber attributes using local-scale metrics from terrestrial LiDAR data: A case study of Newfoundland conifer species. *Forest Ecology and Management* 347: 116-129.
- Burger H., 1939, Der Kronenaufbau gleichalteriger Nadelholzbestände. *Mitteilungen der Schweizerischen Anstalt für das forstliche Versuchswesen* 21(1): 5-57.
- Calders K., Adams J., Armston J., Bartholomeus H., Bauwens S., Bentley L.P., Chave J., Danson F.M., Demol M., Disney M., Gaulton R., Moorthy S.M.K., Levick S.R., Saarinen N., Schaaf C., Stovall A., Terry L., Wilkes P. &

- Verbeeck H., 2020, Terrestrial laser scanning in forest ecology: expanding the horizon. *Remote Sensing of Environment* 251: 112102.
- Campbell S.A. & Borden J.H., 2005, Bark reflectance spectra of conifers and angiosperms: implications for host discrimination by coniferophagous bark and timber beetles. *The Canadian Entomologist* 137: 719–722.
- Cannell M.G.R., 1982, World forest biomass and primary production data. Academic Press, London, 391 pp.
- Colombo S.J., 2008, Ontario's forests and forestry in a changing climate / Climate change research report; CCRR-12. Ontario Forest Research Institute, Ontario Ministry of Natural Resources, 22 pp.
- Dai X., 2021, Novel methods for estimating aboveground biomass. Master Thesis (Forestry). University of New Brunswick, 123 pp. DOI: 10.13140/RG.2.2.13216.30721
- Dalponte M., Bruzzone L. & Gianelle D., 2008, Fusion of hyperspectral and LiDAR remote sensing data for classification of complex forest areas. *IEEE Transactions on Geoscience and Remote Sensing* 46: 1416–1427.
- Dalponte M., 2018, itcSegment: Individual tree crowns segmentation. R package version 0.8. <https://CRAN.R-project.org/package=itcSegment>.
- Danilin I.M., Medvedev E.M. & Melnikov S.R., 2005, Laser location of earth and forest: Textbook. Krasnoyarsk, V.N. Sukachev Institute of forest, Russian Academy of sciences, Siberian branch, 182 pp. (In Russian).
- Dengler A., 1937, Kronengrösse, Nadelmenge und Zuwachsleistung von Altkiefern. *Zeitschrift für Forst- und Jagdwesen* 69: 321-336.
- Falster D.S., Duursma R.A., Ishihara M.I., Barneche D.R., FitzJohn R.G., Vårhammar A., Aiba M., Ando M., Anten N., Aspinwall M.J., Baltzer J.L., Baraloto C., Battaglia M., Battles J.J., Bond-Lamberty B., van Breugel M., Camac J., Claveau Y., Coll L., Dannoura M., Delagrange S., Domec J.-C., Fatemi F., Feng W., Gargaglione V., Goto Y., Hagihara A., Hall J.S., Hamilton S., Harja D., Hiura T., Holdaway R., Hutley L.S., Ichie T., Jokela E.J., Kantola A., Kelly J.W.G., Kenzo T., King D., Kloeppel B.D., Kohyama T., Komiyama A., Laclau J.-P., Lusk C.H., Maguire D.A., le Maire G., Mäkelä A., Markesteijn L., Marshall J., McCulloh K., Miyata I., Mokany K., Mori S., Myster R.W., Nagano M., Naidu S.L., Nouvellon Y., O'Grady A.P., O'Hara K.L., Ohtsuka T., Osada N., Osunkoya O.O., Peri P.L., Petritan A.M., Poorter L., Portsmouth A., Potvin C., Ransijn J., Reid D., Ribeiro S.C., Roberts S.D., Rodríguez R., Saldaña-Acosta A., Santa-Regina I., Sasa K., Selaya N.G., Sillett S.C., Sterck F., Takagi K., Tange T., Tanouchi H., Tissue D., Umehara T., Utsugi H., Vadeboncoeur M.A., Valladares F., Vanninen P., Wang J.R., Wenk E., Williams R., Ximenes F. de Aquino, Yamaba A., Yamada T., Yamakura T., Yanai R.D. & York R.A., 2015, BAAD: a Biomass And Allometry Database for woody plants. *Ecology* 96: 1445–1445.
- Fu L., Sun W. & Wang G., 2017, A climate-sensitive aboveground biomass model for three larch species in northeastern and northern China. *Trees* 31: 557–573.

- Fu W. & Wu Y., 2011, Estimation of aboveground biomass of different mangrove trees based on canopy diameter and tree height. *Procedia Environmental Sciences* 10: 2189–2194.
- Goodman R.C., Phillips O.L. & Baker T.R., 2014, The importance of crown dimensions to improve tropical tree biomass estimates. *Ecological Applications* 24(4): 680–698.
- Goodwin N.R., Coops N.C. & Culvenor D.S., 2006, Assessment of forest structure with airborne LiDAR and the effects of platform altitude. *Remote Sensing of Environment* 103: 140–152.
- Grote R., Kiese R., Grünwald T., Ourcival J.-M. & Granier A., 2011, Modelling forest carbon balances considering tree mortality and removal. *Agricultural and Forest Meteorology* 151: 179–190.
- Hartig R., 1896, Wachstumsuntersuchungen an Fichten. *Forstlich-Naturwissenschaftliche Zeitschrift* 5(1, 3): 1-15, 33-45.
- Hayashi R., 2014, Evaluation of airborne LiDAR as a tool for obtaining sustainable forest management of Maine's forests. *Electronic Theses and Dissertations*. Paper 2223, 64 pp. <http://digitalcommons.library.umaine.edu/etd>.
- Hennessy A., Clarke K. & Lewis M., 2020, Hyperspectral classification of plants: a review of waveband selection generalisability. *Remote Sensing* 12: 113.
- Huang H. & Mayer H., 2007, Extraction of 3D unfoliated trees from image sequences via a generative statistical approach. *Conference: Pattern Recognition, 29th DAGM Symposium, Heidelberg, Germany, September 12-14, Proceedings*: 1-10.
- Hyypä J., Hyypä H., Leckie D., Gougeon F., Yu X. & Maltamo M., 2008, Review of methods of small-footprint airborne laser scanning for extracting forest inventory data in boreal forests. *International Journal Remote Sensing* 29(5): 1339-1366.
- Jaaskelainen T., Silvennoinen R., Hiltunen J. & Parkkinen J.P.S., 1994, Classification of the reflectance spectra of pine, spruce, and birch. *Applied Optics* 33: 2356-2362.
- Jensen J.R., 2005, *Introductory digital image processing*. Third edition. Upper Saddle River, New Jersey, Prentice Hall, 526 pp.
- Jing L., Hu B., Noland T. & Li J., 2012, An individual tree crown delineation method based on multi-scale segmentation of imagery. *ISPRS Journal of Photogrammetry and Remote Sensing* 70: 88–98.
- Jucker T., Caspersen J., Chave J., Antin C., Barbier N., Bongers F., Dalponte M., van Ewijk K.Y., Forrester D.I., Heani M., Higgins S.I., Holdaway R.J., Iida Y., Lorimer C., Marshall P.M., Momo S., Moncrieff G.R., Ploton P., Poorter L., Rahman K.A., Schlund M., Sonké B., Sterck F.J., Trugman A.T., Usoltsev V.A., Vanderwel M.C., Waldner P., Wedeux B., Wirth C., Wöll H., Woods M., Xiang W., Zimmermann N. & Coomes D.A., 2017, Allometric equations for integrating remote sensing imagery into forest monitoring programmes. *Global Change Biology* 23: 177-190.

- Kajihara M., 1981, Crown form, crown structure and the relationship between crown dimensions and leaf fresh weight of hinoki (*Chamaecyparis obtusa*). Bulletin of the Kyoto Prefectural University Forests 25: 11-28.
- Kajihara M., 1980, Crown structure of sugi (*Cryptomeria japonica*) and the relationship between crown dimensions and leaf fresh weight. Bulletin of the Kyoto Prefectural University Forests 24: 49-63.
- Kapustinskaite T.K. & Rusečkas J.J., 1982, Tables for determining the leaf surface and weight of various parts of a tree in forest phytocenoses. Lithuanian Forestry Research Institute, Kaunas, Lithuania, 11 pp. (in Russian).
- Kern K.G., 1962, Die Beziehungen zwischen einigen Kronenkennwerten und dem Nadel Trockengewicht bei Fichte und Tanne. Allgemeine Forst- und Jagdzeitung 133: 13 -18.
- Knight T.C., Ezell A.W., Shaw D.R., Byrd J.D. & Evans D.L., 2004, Identifying loblolly pine and four common competing hardwood species using multispectral reflectance analysis, [in:] K.F. Connor (ed.), Proceedings of the 12th biennial southern silvicultural research conference. Gen. Tech. Rep. SRS-71. Asheville, NC: U.S. Department of Agriculture, Forest Service, Southern Research Station: 336-342.
- Lau A., Calders K., Bartholomeus H., Martius C., Raunonen P., Herold M., Vicari M., Sukhdeo H., Singh J. & Goodman R.C., 2019, Tree biomass equations from terrestrial LiDAR: a case study in Guyana. Forests 10: 527.
- Lefsky M.A., Cohen W.B., Parker G.G. & Harding D.J., 2003, Lidar remote sensing for ecosystem studies. AIBS Bulletin 52(1): 19-30.
- Leontiev V.L., 1950, On the estimation of the biomass of *Haloxylon* Bunge. Botanical Journal [Botanicheskiy Zhurnal] 35(6): 637-645. (in Russian).
- Lines E.R., Zavala M.A., Purves D.W. & Coomes D.A., 2012, Predictable changes in aboveground allometry of trees along gradients of temperature, aridity and competition. Global Ecology and Biogeography 21: 1017–1028.
- Liu R., Yang X., Gao R., Hou X., Huo L., Huang Z. & Cornelissen J.H.C., 2021, Allometry rather than abiotic drivers explains biomass allocation among leaves, stems and roots of *Artemisia* across a large environmental gradient in China. Journal of Ecology 109(2): 1026-1040.
- Luo Y., Wang X., Ouyang Z., Lu F., Feng L. & Tao J., 2020, A review of biomass equations for China's tree species. Earth System Science Data 12(1): 21-40.
- Machimura T., Fujimoto A., Hayashi K., Takagi H. & Sugita S., 2021, A novel tree biomass estimation model applying the pipe model theory and adaptable to UAV-derived canopy height models. Forests 12: 258.
- Martin M.E., Newman S.D., Aber J.D. & Congalton R.G., 1998, Determining forest species composition using high spectral resolution remote sensing data. Remote Sensing of Environment 65: 249–254.
- Mas J.F. & Flores J.J., 2008, The application of artificial neural networks to the analysis of remotely sensed data. International Journal of Remote Sensing 29: 3617–3663.

- Masaitis G., Mozgeris G., Augustaitis A., 2013, Spectral reflectance properties of healthy and stressed coniferous trees. *iForest*: e1-e7. <http://www.sisef.it/iforest/contents?id=ifor0709-006>
- Næsset E. & Økland T., 2002, Estimating tree height and tree crown properties using airborne scanning laser in a boreal nature reserve. *Remote Sensing of Environment* 79: 105–115.
- Næsset E., Gobakken T., Holmgren J., Hyyppä H., Hyyppä J., Maltamo M., Nilsson M., Olsson H., Persson A. & Derman U., 2004, Laser scanning of forest resources: the Nordic experience. *Scandinavian Journal of Forest Research* 19: 482-489.
- Neuville R., Bates J.S. & Jonard F., 2021, Estimating forest structure from UAV-mounted LiDAR point cloud using machine learning. *Remote Sensing* 13: 352.
- Ohmann L.F., Grigal D.F. & Brander R.B., 1976, Biomass estimation for five shrubs from northeastern Minnesota. USDA Forest Service, North Central Forest Experiment Station. Research paper NC-133, 11 pp. https://www.nrs.fs.fed.us/pubs/rp/rp_nc133.pdf
- Oki K., Shan L., Saruwatari T., Suhama T. & Omasa K., 2006, Evaluation of supervised classification algorithms for identifying crops using airborne hyperspectral data. *International Journal of Remote Sensing* 27(10): 1993–2002.
- Ørka H.O., Næsset E. & Bollandsås O.M., 2009, Classifying species of individual trees by intensity and structure features derived from airborne laser scanner data. *Remote Sensing of Environment* 113: 1163–1174.
- Poorter H., Jagodzinski A.M., Ruiz-Peinado R., Kuyah S., Luo Y., Oleksyn J., Usoltsev V.A., Buckley T.N., Reich P.B. & Sack L., 2015, How does biomass allocation change with size and differ among species? An analysis for 1200 plant species from five continents. *New Phytologist* 208(3): 736-749.
- Pozdnyakov L.K., Protopopov V.V. & Gorbatenko V.M., 1969, Biological productivity of forests in Middle Siberia and Yakutia. Knizhnoe Izdatelstvo, Krasnoyarsk, 120 pp. (in Russian).
- Puttonen E., Litkey P. & Hyyppä J., 2010, Individual tree species classification by illuminated—shaded area separation. *Remote Sensing* 2: 19-35.
- Puttonen E., Jaakkola A., Litkey P. & Hyyppä J., 2011, Tree classification with fused mobile laser scanning and hyperspectral data. *Sensors* 11(5): 5158–5182.
- Rehling F., Sandner T.M. & Matthies D., 2021, Biomass partitioning in response to intraspecific competition depends on nutrients and species characteristics: a study of 43 plant species. *Journal of Ecology*. Preprint. DOI:10.1111/1365-2745.13635.
- Schepaschenko D., Shvidenko A., Usoltsev V.A., Lakyda P., Luo Y., Vasylyshyn R., Lakyda I., Myklush Y., See L., McCallum I., Fritz S., Kraxner F. & Obersteiner M., 2017, A dataset of forest biomass structure for Eurasia. *Scientific Data* 4 (No 170070): 1-11.
- Shlyakhter I., Rozenoer M., Dorsey J. & Teller S., 2001, Reconstructing 3D tree models from instrumented photographs. *IEE Computer Graphics and Applications* 21(3): 53–61.

- Sobhan I., 2007, Species discrimination from a hyperspectral perspective. Doctoral Thesis. International Institute for Geoinformation Science & Earth Observation, Enschede, the Netherlands, 164 pp.
- Tolkach I.V. & Sayevich F.K., 2016, Spectral and brightness characteristics of the main forest-forming species on images of the scanner Leica ADS100. Proceedings of Belarusian State Technological University 1: 24-27. (in Russian).
- Usoltsev V.A., 2016, Single-tree biomass of forest-forming species in Eurasia: Database, climate-related geography, weight tables. Ural State Forest Engineering University, Yekaterinburg, 336 pp. <https://elar.usfeu.ru/handle/123456789/5696>
- Usoltsev V.A., 2020, Single-tree biomass data for remote sensing and ground measuring of Eurasian forests: digital version. The second edition, enlarged. Ural State Forest Engineering University; Botanical Garden of Ural Branch of RAS, Yekaterinburg. https://elar.usfeu.ru/bitstream/123456789/9647/2/Base1_v2_ob.pdf
- Usoltsev V.A., Shobairi S.O.R. & Chasovskikh V.P., 2019a, Comparing of allometric models of single-tree biomass intended for airborne laser sensing and terrestrial taxation of carbon pool in the forests of Eurasia. Natural Resource Modeling 32: e12187.
- Usoltsev V.A., Zukow W., Osmirko A.A., Tsepordey I.S. & Chasovskikh V.P., 2019b, Additive biomass models for *Quercus* spp. single-trees sensitive to temperature and precipitation in Eurasia. Ecological Questions 30(4): 29–40.
- Usoltsev V.A., Shobairi O., Tsepordey I.S., Ahrari A., Zhang M., Shoaib A.A. & Chasovskikh V.P., 2020a, Are there differences in the response of natural stand and plantation biomass to changes in temperature and precipitation? A case for two-needled pines in Eurasia. Journal of Resources and Ecology 11(4): 331–341.
- Usoltsev V.A., Shobairi O., Tsepordey I.S. & Chasovskikh V.P., 2020b, On some differences in the response of *Picea* spp. and *Abies* spp. single-tree biomass structure to changes in temperatures and precipitation in Eurasia. Environment and Ecology 38(3): 300–315.
- Van den Berge S., Vangansbeke P., Calders K., Vanneste T., Baeten L., Verbeeck H., Parvathi S., Moorthy K. & Verheyen K., 2021, Biomass expansion factors for hedgerow-grown trees derived from terrestrial LiDAR. BioEnergy Research (Preprint). DOI: 10.1007/s12155-021-10250-y
- Veyisov S. & Kaplin V.G., 1976, To the method of biomass estimating in white saxaul of the Eastern Kara-Kum desert. Problems of desert exploitation [Problemy osvoeniya pustyn'] 1: 60–64. (in Russian).
- Voss M. & Sugumaran R., 2008, Seasonal effect on tree species classification in an urban environment using hyperspectral data, LiDAR, and an object-oriented approach. Sensors 8: 3020–3036.
- Westman W.E. & Whittaker R.H., 1975, The pygmy forest region of Northern California: studies on biomass and primary productivity. The Journal of Ecology 63: 493-520.
- World Weather Maps, 2007. <https://www.mapsofworld.com/referrals/weather>

- Xiong F., Nie X., Yang L., Wang L., Li J. & Zhou G., 2021, Biomass partitioning pattern of *Rheum tanguticum* on the Qinghai–Tibet Plateau was affected by water-related factors. *Plant Ecology*. Preprint. DOI:10.1007/s11258-021-01122-8
- Zanotelli D., Montagnani L., Manca G. & Tagliavini M., 2013, Net primary productivity, allocation pattern and carbon use efficiency in an apple orchard assessed by integrating eddy covariance, biometric and continuous soil chamber measurements. *Biogeosciences* 10: 3089–3108.
- Zeng W.S., Duo H.R., Lei X.D., Chen X.Y., Wang X.J., Pu Y. & Zou W.T., 2017, Individual tree biomass equations and growth models sensitive to climate variables for *Larix* spp. in China. *European Journal of Forest Research* 136: 233–249.
- Zhang C. & Qiu F., 2012, Mapping individual tree species in an urban forest using airborne lidar data and hyperspectral imagery. *Photogrammetric Engineering & Remote Sensing* 78(10): 1079–1087.
- Zhang K. & Hu B., 2012, Individual urban tree species classification using very high spatial resolution airborne multi-spectral imagery using longitudinal profiles. *Remote Sensing* 4: 1741-1757.
- Zhen Z., Quackenbush L.J. & Zhang L., 2016, Trends in automatic individual tree crown detection and delineation—Evolution of LiDAR data. *Remote Sensing* 8(4): 333.